DWDM millimeter-wave radio-on-fiber systems

Hiroyuki Toda[a], Toshiaki Kuri[b], and Ken-ichi Kitayama[c]
[a]Faculty of Engineering, Doshisha University, Kyotanabe, Kyoto, Japan 610-0321;
[b]National Institute of Information and Communications Technology, Tokyo, Japan 184-8795;
[c]Osaka University, Osaka, Japan 565-0871

ABSTRACT

We describe some of our recent results on DWDM mm-wave radio-on-fiber (RoF) technology for future broadband wireless systems. A supercontinuum (SC) light source is a promising multiwavelength light source for the system with photonic up-conversion. Multiplexing and demultiplexing schemes for optical frequency interleaving in order to extend the number of antenna base stations can be constructed using a properly designed arrayed-waveguide grating (AWG). We demonstrate a full-duplex WDM mm-wave RoF system using a SC light source. The periodic nature of AWG, where the period is free spectral range (FSR), is used for utilizing the full bandwidth of the SC light source. Half of the SC output modes are used for downlink transmission with photonic upconversion. Another half of the SC output modes are used for uplink transmission with photonic downconversion. These techniques are effective to use a wealth of optical frequency resources from the SC light source. Two-channel downlink and one-channel uplink 60-GHz band RoF signals were simultaneously transmitted over 25-km standard single-mode fiber with error-free and no noticeable power penalty.

Keywords: radio on fiber, millimeter wave photonics, optical fiber communication, dense wavelength division multiplexing (DWDM), arrayed waveguide grating, subcarrier multiplexing, optical waveguide components, supercontinuum

1. INTRODUCTION

Radio on Fiber (RoF) is a technique where an optical carrier is modulated by RF wireless signals and transmitted through optical fibers to take advantage of their broad bandwidth and the low propagation loss [1-4]. The advantages of the RoF systems constructed by a central station (CS) and base stations (BSs) with antenna include simple BS configuration, centralized operation, easy maintenance and low consumption power. A lot of efforts have been dedicated to realize practical microwave wireless systems using the RoF technique. The RoF systems are also very attractive for future millimeter-wave (mm-wave) broadband wireless systems because the number of BS becomes huge due to the large free-space propagation loss of the mm-wave.

One of the promising ways to support a large number of BSs is to assign a wavelength to each BS using the dense wavelength division multiplexing (DWDM) technique [5-7]. A possible configuration of the DWDM RoF for inbuilding wireless network is shown in Fig. 1 [8]. The DWDM technology developed for large capacity digital baseband transmission systems can be applied to such mm-wave RoF systems. In this paper, we describe our recent results of DWDM mm-wave RoF systems.

We first show the principle of the frequency interleaved DWDM radio-on-fiber in Sec. 2. The optical frequency interleaving improves the optical spectral efficiency of DWDM RoF systems. The possible configurations of multiplexing (MUX) and demultiplexing (DEMUX) schemes using an AWG are described. In Sec. 3, we propose to use a supercontinuum (SC) light source for RoF systems as a multiwavelength light source. In Sec. 4, a bus link configuration using a periodic nature of AWG is described. In Sec. 5, full-duplex experiment is described. Finally we conclude this paper in Sec. 6.

2. OPTICAL FREQUENCY INTERLEAVING

A. Concept

In conventional wireless systems, the bandwidth of the RF signal is much narrower than the RF carrier frequency. Therefore, the optical spectral efficiency becomes quite low in DWDM RoF systems. Fig. 2 (a) shows an example of optical spectrum. In this figure, we assume that the carrier frequency of the mm-wave signal is in 60 GHz band, the channel separation is a multiple (1, 2, 4, 8…) of 25 GHz, and the optical modulation format is SSB. The minimum channel separation in this case is 100 GHz, where large portion of optical frequency is unused. To increase the spectral efficiency of the system, the concept of optical frequency interleaving was first proposed by Schäffer et al. in simultaneous up-conversion scheme with an electro-optic modulator [9]. Fig. 2 (b) shows the optical spectrum of the frequency interleaved DWDM RoF signals [10-12]. The optical spectral efficiency can be improved by 4 times even if the 60-GHz band (59.0 - 66.0 GHz in Japanese frequency assignment plan) is fully utilized. When the bandwidth of the mm-wave signal is several hundred MHz, sub-GHz channel separation might be ultimately possible if ultra-narrowband demultiplexing filters and highly stable laser sources are obtained. Using the frequency interleaving, 300 full-duplex BSs can be supported in a fiber pair when available optical bandwidth is 75 nm (C and L bands) [13].

B. Multiplexing/demultiplexing scheme using an AWG

In this subsection, we describe possible configurations of multiplexing and demultiplexing the optical frequency interleaved DWDM RoF signals.

Fig. 3 (a) shows a configuration of the multiplexing scheme which consists of an AWG with N input and 2 output waveguides (N x 2 AWG), where N is the total channel number of RoF signals, and an optical variable coupler (VC) [14]. The AWG is designed to filter the carriers and single sidebands of input RoF signals to the output waveguides, respectively, as shown in Fig. 3 (b). This can be done by properly adjusting the position and the separation of the input and output waveguides at the interfaces between the channel waveguides and slab waveguide regions [15]. The filtered carriers and sidebands shown in B and C of Fig. 3 (b) are combined by the VC. The modulation indices of the multiplexed RoF signals can be simultaneously controlled simply by changing the coupling ratio of the VC. Also noted that this scheme operates not only as a frequency interleaved DWDM multiplexer but also as optical SSB filters for RoF signals of all the channels.

Fig. 4 shows a configuration of the demultiplexing scheme, which consists of a high-finesse Fabry-Perot etalon (FP), an optical circulator (OC), and an AWG with 2-input and N-output waveguides (2 x N AWG, N: total channel number) [16]. The free spectral range of the FP is adjusted to the channel spacing *Df* in order to separate optical carriers (transmission; the spectrum is the same as B of Fig. 3 (b)) and sidebands (reflection; C of Fig. 3 (c)) from the multiplexed RoF signals. The AWG is exactly the same configuration as the one used in the multiplexer with reverse order. As a result, the carrier and the sideband, both of the desired channel are filtered to the desired output of the 2 x N AWG.

In the 2-channel transmission experiment with 25-GHz channel spacing [16], two N x 1 AWGs with 25-GHz spacing were used and combined in parallel for the multiplexing operation since the proposed N x 2 AWG is not available. Each AWG is tuned so that the carriers or the sidebands of input RoF signals are filtered out to the output waveguides, respectively. No noticeable power penalty was observed in the received 156 Mbps data due to 25-km SMF transmission and interchannel interference. The receiver sensitivity was improved by 6 dB by optimizing the modulation index of the RoF signal.

3. USE OF SUPERCONTINUUM LIGHT SOURCE

A supercontinuum (SC) light source, which generates broadband optical frequency comb by means of optical nonlinearities of a properly designed fiber, has been energetically developed to realize space-saving and low cost transmitter for DWDM digital baseband transmission systems [17-19].

In DWDM RoF systems, a compact light source should also be a crucial issue in order to realize a practical CS [20]. Thus, we recently proposed to use a SC light source as a multiwavelength light source for DWDM mm-wave RoF systems [21-23]. The SC light source used in our experiment is NTT Electronics, NIESP-SC-001, where the configuration is shown in Fig. 5. The SC modes, where the separation is 25 GHz, are ranging from 1534 nm to 1599 nm with +/– 5 dB flatness, except for several nanometers around the seed laser wavelength (1565 nm). The output

power of the individual SC mode around 1552 nm and the total output power of the SC light source is – 8 dBm and + 22 dBm, respectively.

In order to qualify the SC light source as the multiwavelength light source for DWDM mm-wave RoF systems, the single-sideband (SSB) phase-noise characteristics of 50-GHz beat signals generated by using a 25-GHz-spacing SC light source were evaluated [21, 22]. The results summarized in Table 1 shows that the SC light source meets the requirements for DWDM RoF systems.

Table1: Comparison of SSB phase noise (dBc/Hz) [21, 22]

offset frequency	1 kHz	10 kHz	100 kHz
measured 50-GHz beat of SC	- 78.6	- 96.1	- 100.1
typical 50-GHz synthesized generator	- 60	- 68	- 89

4. BUS-LINK CONFIGURATION USING A PERIODIC NATURE OF AWG PLACED AT A NODE

Fig.6 illustrates a downlink configuration of a WDM mm-wave-band RoF system using a single SC light source. Individual SC mode, whose frequency is denoted by f_n (n: integer number), is extracted by a demultiplexer (DEMUX: AWG1). The frequency interval f_G of the SC comb reported so far ranges in microwave and millimeter wave regions (between 5 GHz and 50 GHz). Therefore, the photonic up- or down-conversion technique [24] can be employed, which eliminates need for mm-wave components in the CS. In the figure, we employ the photonic up-conversion technique, where the optical modes at f_{4i+1} (i: integer number) are modulated by IF data independently. An f_G-spaced DEMUX (AWG3), where the free spectral range (FSR) is denoted by f_{FSR}, which is a multiple of f_G, is placed at a node. This DEMUX feeds the RoF signals separated by f_{FSR} to each bus link. Each RoF signal can be extracted by a fiber Bragg grating (FBG) filter. By using the periodic nature of the AWG, where the period is FSR, the size of AWG3 can be smaller even when the full bandwidth of the SC light source is used. Also each BS does not need to be connected to the node individually, which greatly saves the total fiber length for the BSs. Note that the periodic nature of AWG1 and AWG2 may be able to be used in the CS in conjunction with FBG filters in order to save the complexity of the AWGs.

In this example, only odd number of the SC modes are used for downlink. This is because 50-GHz spaced SC modes suit well for photonic upconversion to generate 60-GHz RoF signals, while the SC mode spacing is 25 GHz. Therefore, we propose to use the rest of the SC modes for uplink to realize a full-duplex RoF system.

5. FULL DUPLEX CONFIGURATION WITH PHOTONIC UP- AND DOWNCONVERSION

A. Experimental setup and operation principle

Fig. 7 shows the experimental setup for the full duplex configuration. In the experiment, we will show transmission of two downlink channels and one uplink channel simultaneously. Fig. 8 shows conceptional optical spectra of (a); SC outputs, (b); after modulation, (c); AWG 3 output, and (d); PD1 input, respectively. D and U indicate downlink and uplink, respectively. Modulation was performed by 9.6-GHz IF signal carrying a 156 Mbps DPSK data with $LiNbO_3$ Mach-Zehnder modulators (LNMs). The FSR of the AWG3 used in the experiment was f_m = 0.80 THz (= 6.4 nm at 1550 nm). Fig. 9 shows optical spectra for uplink signal. The 50-GHz spaced even number SC modes f_2 and f_4 are filtered by AWG3 (Fig. 7 (e)). The two SC modes are simultaneously intensity modulated with an electro-absorption modulator (EAM) by 60-GHz mm-wave signal carrying 156 Mbps DPSK data (Fig. 7 (f)). Finally the carrier f_2 and single sideband f_2 - f_{IF} is filtered by narrow band FBG2 and photodetected by PD4. Here, photonic downconversion [7] allows us to detect 10-GHz IF signal after photodetection of the 60-GHz RoF signal.

The AWG1 and AWG2 were tuned by temperature to the SC modes. The carrier wavelengths of the downlink channels 1 and 2 are 1546.7 and 1553.1 nm, respectively. The 3-dB bandwidths of FBG1 and FBG2 are 1.4 nm and 0.2 nm, respectively. Finally, the bit-error rates (BERs) of the decoded 156-Mbps data for up- and downlink transmission are measured.

B. Downlink results

Here we present the results of downlink transmission. Note that all signals (two downlink and one uplink) are transmitted simultaneously during the experiment in order to clarify full-duplex operation. Fig. 10 shows the measured optical spectra of the two RoF signals (channels 1 and 2) detected at the FBG1 outputs. Separation between the carrier and the desired sideband is 60 GHz as indicated by arrows. From these spectra, one can estimate the mm-wave signal level of the undesired channel to be suppressed by about - 35 dB and - 28 dB of the desired signal level for channels 1 and 2.

We measured the BERs of channels 1 and 2 versus the received optical power. Fig. 11 plots the results. As shown in the figure, the error-free transmission (BER < 10^{-9}) for both channels are simultaneously achieved. The difference in the optical receiver sensitivity may be attributed to the difference of carrier to sideband ratio (CSR). Here, CSR means the power difference between the optical carrier and the 60 GHz sideband. The power penalty of less than 0.5 dB was observed after 25-km SMF transmission. This is because that the undesired sideband of the RoF signal is effectively suppressed by the AWG. Therefore, the RoF signal is free from the signal fading problem due to the chromatic dispersion of the transmission fiber.

C. Uplink results

Fig. 12 shows optical spectra, which corresponds to (a), (b) and (c) of Fig. 4. Even though the considerable amount of crosstalk can be seen in the figure due to the crosstalk of the AWGs, One can see that this crosstalk does not influence so much on the receiver performance since the beat signals due to the crosstalk is out of 10 GHz band. Fig. 13 shows measured BER versus received optical power, which is defined as the optical input power of pre-EDFA for PD4 in Fig. 2. As shown in Fig. 2, we used an EDFA in front of EAM because the optical power to the pre-EDFA was slightly less than the power needed for error-free operation. Since one does not want to put an EDFA at this position, we should analyze power diagram of the system to remove this EDFA in future. Nevertheless, error free transmission was obtained as seen in the figure. No noticeable power penalty was observed after 25-km SMF transmission. This is once again because that the undesired sideband component of the RoF signal is effectively suppressed by AWGs and FBG2.

6. CONCLUSION

Recent results of DWDM mm-wave RoF systems for future broadband wireless systems were described. A supercontinuum light source is a promising multiwavelength light source for the system with photonic up- and down-conversion because of its broad bandwidth and the low phase noise of the mm-wave beat. Optical frequency interleaving which improves the optical spectral efficiency is effective to extend the number of BSs, where multiplexing and demultiplexing schemes can be constructed using a properly designed arrayed-waveguide grating.

ACKNOWLEDGMENTS

The authors would like to thank Mr. T. Yamashita and T. Nakashotani for their devoted efforts to the experiment. This research was supported by "Support system for R&D activities in info-communications area" conducted by Telecommunications Advancement Organization of Japan (TAO).

REFERENCES

[1] C. H. Cox, “Analog Optical Links: Theory and Practice,” Cambridge University Press, 2004.
[2] Special Issue on Radio over Fibre Systems, *Fiber and Integrated Optics*, vol. 19, no. 2, 2000.
[3] Special Issue on Microwave Photonics, *IEEE J. Lightwave Technol.*, vol. 21, no. 12, 2003.
[4] Symposium on Photonics in Wireless Systems, *Proc of ECOC 2004*, no. 5, We3.1 and Th1.1, pp. 106-135, Stockholm, 2004.
[5] K. Kitayama, T. Kuri, K. Onohara, T. Kamisaka, and K. Murashima, *IEEE/OSA J. Lightwave Technol.*, vol. 20, p. 1397, 2002.
[6] A. Narasimha, X. Meng, C. F. Lam, M. C. Wu, and E. Yablonovitch, *IEEE Trans. Microwave Theory Tech.*, vol. 49, p. 2042, 2001.

[7] C. Lim, A. Nirmalathas, M. Attygalle, D. Novak, and R. Waterhouse, *IEEE/OSA J. Lightwave Technol.*, vol. 21, p. 2203, 2003.
[8] T. Kuri, K. Ikeda, H. Toda, K.-I. Kitayama, and Y. Takahashi, *LEOS2004*, MF3, Rio Mar , 2004.
[9] C. G. Schäffer, M. Sauer, K. Kojucharow, and H. Kaluzni, *International Topical Meeting on Microwave Photonics*, WE2.4, p. 164, Oxford (2000).
[10] C. Lim A. Nirmalathas, D. Novak, R. S. Tucker, and R. B. Waterhouse, *Electron. Lett.*, vol. 37, p. 1043, 2001.
[11] H. Toda, T. Yamashita, K.-I. Kitayama, and T. Kuri, *MWP2001*, Tu-3.3, p. 85 (postponed to 2002).
[12] C. Lim, A. Nirmalathas, D. Novak, and R. Waterhouse, *IEEE/OSA J. Lightwave Technol.*, vol. 21, p. 3308, 2003.
[13] T. Kuri, H. Toda, and K.-I. Kitayama, *IEEE/OSA J. Lightwave Technol*, vol. 21, p. 1510, 2003.
[14] H. Toda, T. Yamashita, K.-I. Kitayama, and T. Kuri, *MWP2003*, 287 and *ECOC-IOOC2003*, vol. 4, p. 910, 2003.
[15] H. Toda, T. Yamashita, T. Kuri, and K. Kitayama, *IEEE/OSA J. Lightwave Technol*, vol. 21, p. 1735, 2003.
[16] H. Toda, T. Yamashita, K.-I. Kitayama, and T. Kuri, *MWP2002*, W3.4 and *ECOC2002*, 8.2.4, 2002.
[17] K. Mori, H. Takara, and Satoki Kawanishi, *J. Opt. Soc. Amer. B*, vol. 18, p. 1780, 2001.
[18] H. Takara, T. Ohara, K. Mori, K. Sato, E. Yamada, Y. Inoue, T. Shibata, M. Abe, T. Morioka, and K.-I. Sato, *Electron. Lett.*, vol. 36, p. 2089, 2000.
[19] K. Mori, K. Sato, H. Takara, and T. Ohara, *Electron. Lett.*, vol. 39, p. 544, 2003
[20] T. Kuri and K. Kitayama, *IEEE Trans. Microwave Theory Tech.*, 47, 570, 1999.
[21] T. Kuri, T. Nakasyotani, H. Toda, and K.-I. Kitayama, *MWP2004*, MC-2, 40 and *ECOC2004*, Tu3.5, 2004.
[22] T. Kuri, T. Nakasyotani, H. Toda, and K.-I. Kitayama, *IEEE Photon. Tech. Lett.*, vol. 17, p. 1274, 2005.
[23] H. Toda, T. Nakasyotani, T. Kuri, and K.-I. Kitayama, *MWP2004*, TA-2, 161 and *ECOC2004*, We4.P.158, 2004.
[24] H. Toda, T. Nakasyotani, T. Kuri, and K.-I. Kitayama, *International Topical Meeting on Microwave Photonics (MWP2004)*, TA-2, pp. 161-164, Ogunquit, Oct. 2004.

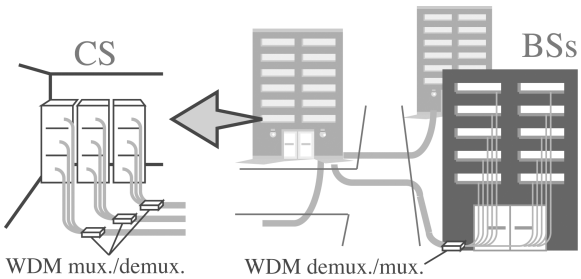

Fig. 1 A possible configuration of DWDM RoF for an in-building wireless network [8]. CS: central station, BS: base station.

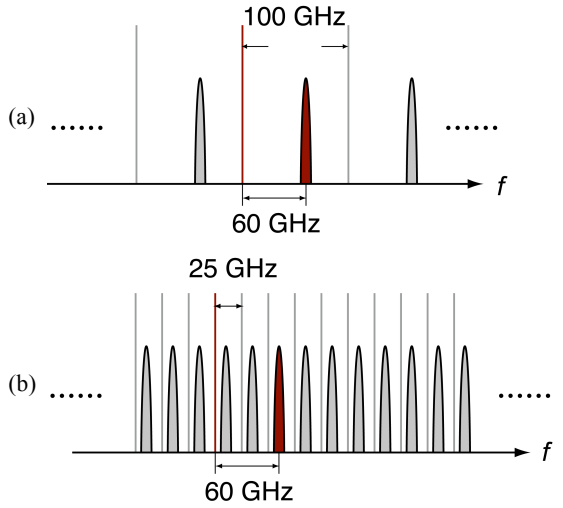

Fig. 2 Optical spectra of DWDM mm-wave RoF signals without (a) and with (b) optical frequency interleaving. Optical modulation format is assumed to be SSB.

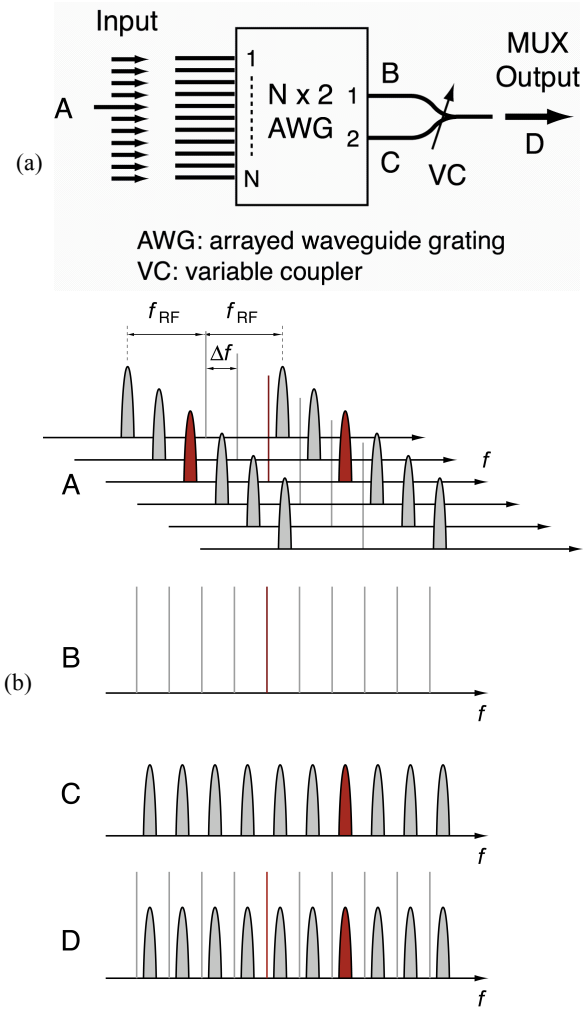

Fig. 3 (a) Configuration of a multiplexing scheme. (b) Optical frequency spectra of A; one of the input channels (optical DSB), B and C; filtered carriers and single sidebands by N x 2 AWG, and D; multiplexed output by variable coupler VC. f_{RF} and Df are the mm-wave carrier frequency and the channel separation, respectively. Note that this scheme also operates as optical SSB filters.

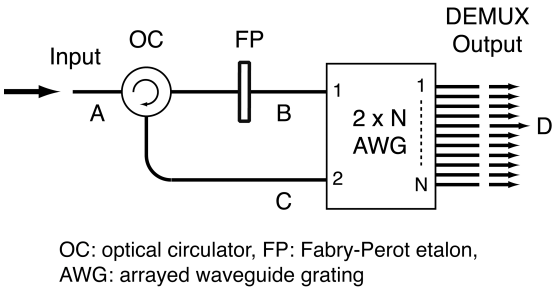

Fig. 4 Configuration of a demultiplexing scheme. The AWG is the same as the one used in the multiplexing scheme with reverse order.

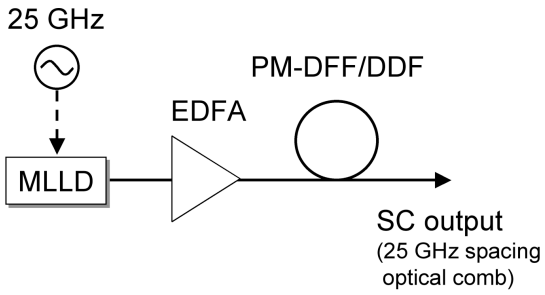

MLLD: mode-locked laser diode, PM-DFF/DDF: polarization-maintaining dispersion-flattened dispersion-decreasing fiber

Fig. 5 Configuration of the SC light source used in the experiment.

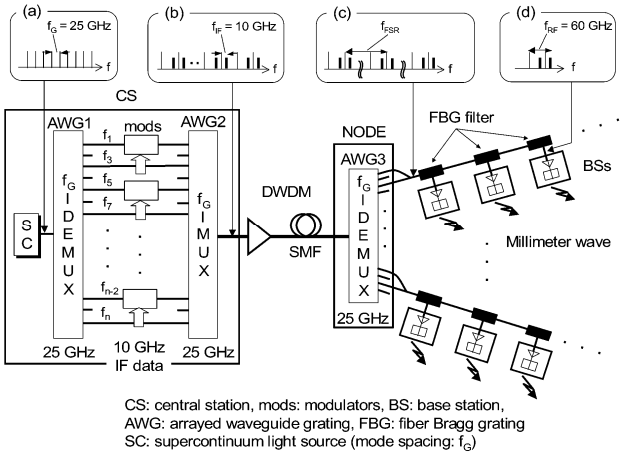

Fig. 6 A downlink configuration of a DWDM mm-wave RoF using a single SC light source for the multiwavelength light source. Photonic up-conversion is employed in order to exploit the full potential of the broadband SC light source.

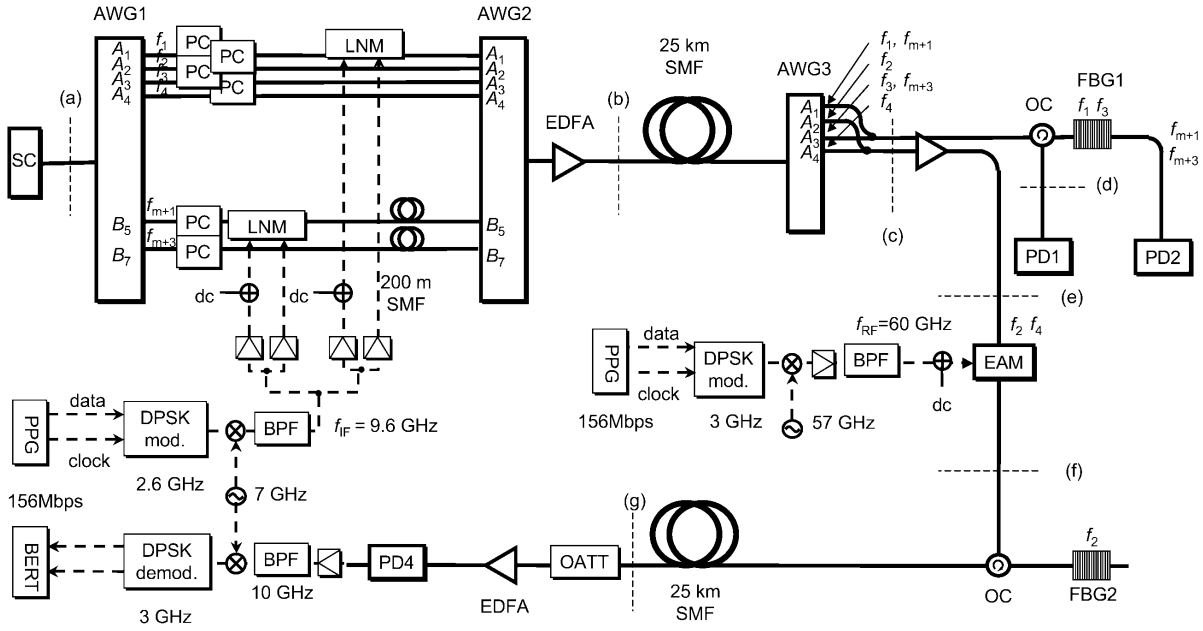

Fig. 7 Experimental setup for the full duplex configuration. In the experiment, two downlink channels and one uplink channel are transmitted simultaneously.

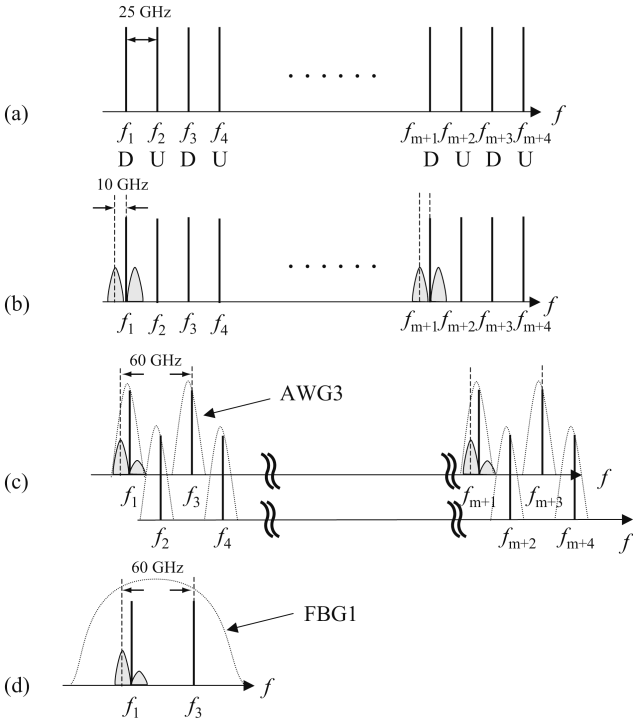

Fig. 8 Conceptional optical spectra of (a); SC outputs, (b); after modulation, (c); AWG 3 output, and (d); PD1 input. D and U indicate downlink and uplink, respectively.

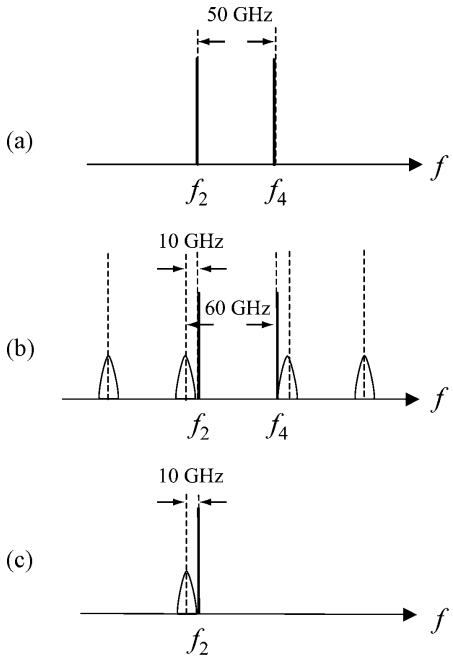

Fig. 9 Optical spectra for uplink signal. (a); 50-GHz spaced two SC modes for the uplink signal (EAM input), (b); after modulation by 60 GHz mm-wave signal (EAM output), and (c); reflection of FBG2 (PD4 input). Photonic downconversion allows us to detect 10-GHz IF signal after photodetection.

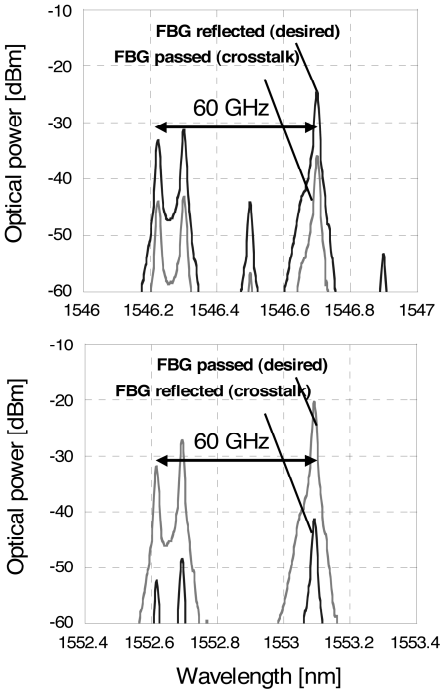

Fig. 10 Measured optical spectra of the two downlink RoF signals at FBG1 outputs: (a) channel1 and (b) channel2.

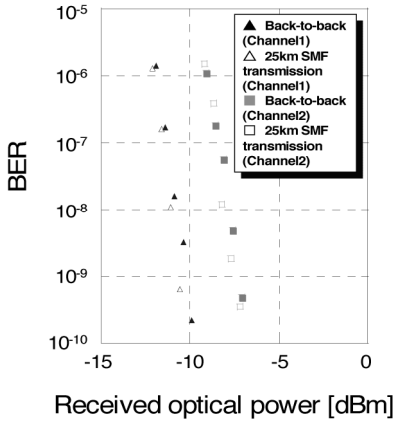

Fig. 11 Measured BERs for downlink RoF signals as a function of received optical power.

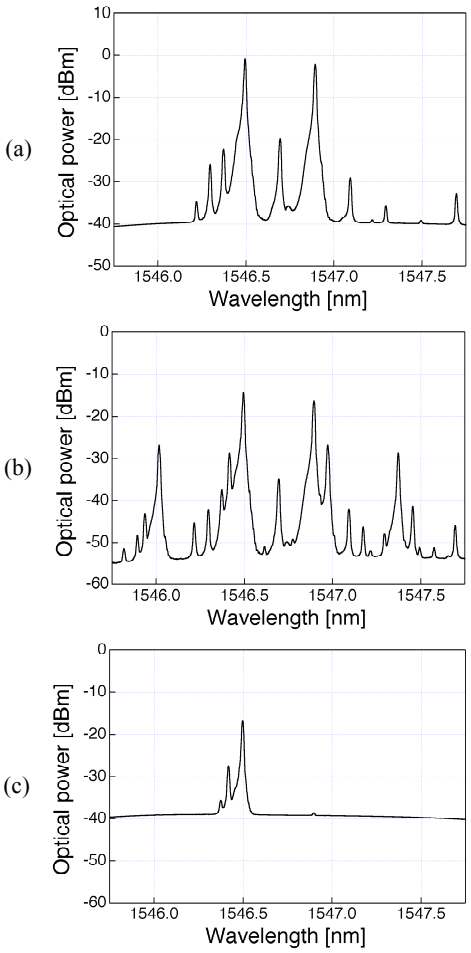

Fig. 12 Measured optical spectra of the uplink RoF signal which corresponds to (a), (b) and (c) of Fig. 9.

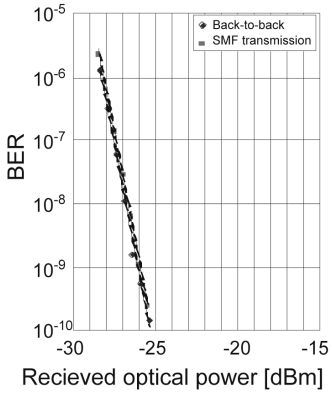

Fig. 13 Measured BERs for the uplink RoF signal as a function of received optical power.